

*Full Length Research Paper*

# **Assessment of the LMDZ model to the dynamic and thermodynamic properties of cyclogenesis in the tropical Atlantic Ocean and on the West African coast**

**Dame Gueye<sup>1</sup>, Abdou Lahat Dieng<sup>2</sup>, Abdoulaye Deme<sup>1\*</sup>, Mouhamadou Bamba Sylla<sup>3</sup> and Abdou Aziz Coly<sup>1</sup>**

<sup>1</sup>LEITER, Applied Science and Technology Training and Research Unit, Gaston University, BP 234, Saint-Louis 32000, Senegal.

<sup>2</sup>LPAOSF, Polytechnic School, Cheikh Anta Diop University, BP 5085, Dakar 10700, Senegal.

<sup>3</sup>African Institute for Mathematical Sciences (AIMS), KN3 Street Kigali, Rwanda.

Received 15 August, 2023; Accepted 23 October, 2023

The study's primary objective is to evaluate the LMDZ model's capacity to simulate the cyclogenesis process, interannual variability of cyclone activity, and associated processes in the tropical Atlantic, focusing on the West African coasts to the central tropical Atlantic region. Two main approaches are used. Firstly, the model's ability to capture the interannual variability in Atlantic cyclogenesis activity is examined through seasonal mean. These seasonal average conditions were identified based on ERAI, along with years characterized by strong and low cyclonic activities. Secondly, a more descriptive approach is undertaken, involving the spatiotemporal monitoring of the Hurricane Karl, which originated near the Cape Verdean coasts on September 16th, 2004, until its dissipation. Horizontal sections of the tropospheric layers most sensitive to the cyclonic phenomenon are used to comprehensively track its progress. The results show a significant variability of cyclonic activity in the tropical Atlantic at different time scales, indicating that the period from July to September and the region along the Intertropical Convergence Zone (ITCZ) are favorable for tropical cyclogenesis. It also revealed that the years of high cyclonic activity are mainly characterized by low sea level pressure, strong 850 hPa relative vorticity, high 700 hPa relative humidity, and strong 200 hPa divergence anomalies, whereas the opposite is observed during the low activity years. The LMDZ model performs well in reproducing cyclonic parameters from the surface to the upper troposphere with mean absolute errors being less important from the surface (11%) to the high troposphere (17%). At the synoptic scale, the model accurately replicates hurricane characteristics, including intensity categories, spatial distribution, and trajectories. However, it falls short in accurately representing the genesis phase, such as tropical depression.

**Key words:** Cyclogenesis, interannual variability, cyclonic activity, tropical depression.

## **INTRODUCTION**

The troposphere, the lowest layer of earth's atmosphere, where various meteorological events like fog, thunderstorms, tornadoes, and cyclones occur. While

these events are essential for providing precipitation for human activities, they can also pose significant public danger.

Tropical cyclones, highly destructive natural disasters causing significant human and property loss, rely on specific conditions for their formation. These cyclones usually originate near the intertropical convergence zone (ITCZ), characterized by low pressure, where trade winds from different hemispheres converge. Notably, in the tropical Atlantic, major cyclones (Category 3 to 5) account for more than 70% of natural damage in the United States (Landsea, 1993).

They can then cause loss of life and property when they evolve near the coast. For example, Hurricane Katrina in 2005 was one of the strongest hurricanes in US history, resulting in approximately 1,836 deaths and causing damage estimated at more than \$108 billion. In Senegal, Tropical Storm Cindy led to the death of several Senegalese fishermen in 1999 (Sall and Sauvageot, 2005). More recently, hurricane Fred, which passed through the Cape Verde Islands in 2015, caused damage on seven out of ten islands and also affected Senegal's coastline, resulting in fatalities associated with a fishing vessel (Jenkins et al., 2017).

The intensification of hurricanes, coupled with their higher frequency due to climate change (Goldenberg et al., 2001), underscores the growing impact of these storms. Climate change is increasingly recognized for amplifying hurricane strength and their capacity for increased rainfall, posing a significant threat to vulnerable regions. To mitigate the far-reaching consequences, our primary defences include observation, understanding, forecasting, and early warning systems. Progress in these areas is vital for more effective planning, risk reduction, and the protection of human lives and property. Climate models, offering reliability, play a pivotal role in advancing these efforts.

Climate models play a crucial role in understanding earth's climate and predicting future climate changes. They incorporate the laws of physics, chemistry, and fluid dynamics, including interactions between the ocean, atmosphere, and surfaces at different time and space scales that significantly impact climate sensitivity (Pohl, 2017). LMDZ is an atmospheric general circulation model (GCM) developed by the 'Laboratoire de Météorologie Dynamique' (LMD, where "Z" refers to the regional refinement capability of the grid or Zoom) of 'Centre National de la Recherche Scientifique' (CNRS). It is used as the atmospheric component of the integrated earth system model at 'Institut Pierre Simon Laplace' (IPSL). The model contributes significantly to the climate change projections used to inform Intergovernmental Panel on Climate Change (IPCC) reports (Hourdin et al., 2006). The simulations used in this study are simulations with

the new physic version of the LMDZ model (LMDZ5). These simulations are used in model intercomparison projects, namely the Atmospheric Model Intercomparison Project (AMIP), which tests all the parameterizations coupled to large-scale dynamics.

Multiple research studies have explored the LMDZ model's performance in West Africa, particularly in various aspects of atmospheric physics. For example, Senghor et al. (2017) delved into the processes governing Saharan dust's vertical distribution. Their work contributed to quantifying the impact of different mechanisms on the seasonal variations of mineral particle distribution in West Africa and the Tropical Atlantic Ocean. The LMDZ model played a pivotal role in identifying the primary physical drivers behind the distinct seasonal patterns in surface dust concentrations and integrated column concentration cumulants. Diallo (2012) focused on understanding the interactions between atmospheric and surface convection and how they influence energy balances. Through both unconstrained and guided simulations, they established feedback connections between convection and monsoon circulation. Additionally, within the "Analyse Multidisciplinaire de la Mousson Africaine" (AMMA) campaign in West Africa, Sane (2011) sets out to assess and validate new model parameterizations, particularly in their ability to represent the life cycle of convective systems. This encompassed dynamic facets of the monsoon, cloud formations, and rainfall patterns. Results indicated that the model effectively mirrored the diurnal cycle of local systems, resembling observed diurnal patterns. However, it fell short in replicating the propagation of convective systems. Furthermore, recent research employing high-resolution GCMs different to LMDZ, has explored cyclone reproduction, forecasting, and climate simulation. These studies (Ohfuchi et al., 2004; Shen et al., 2006; Chauvin et al., 2006; Oouchi et al., 2006) have demonstrated the models' capacity to accurately replicate the intricate circulation patterns and the intensity of tropical cyclones.

In light of the LMDZ model's demonstrated success in various domains, it becomes pertinent to extend its evaluation to more complex phenomena, particularly with regards to cyclonic activity variability and related processes. These intricate facets present a substantial challenge, distinct from the previously explored topics. They offer a rigorous examination of the model's capabilities and its potential utility in comprehensive climate research. Furthermore, they provide insights into representing cyclonic systems across synoptic and mesoscale dimensions, along with the features of the

\*Corresponding author. E-mail: [abdoulaye.deme@ugb.edu.sn](mailto:abdoulaye.deme@ugb.edu.sn). Tel: +221-764149737.

## West African Monsoon.

Motivated by these considerations, this study aims to assess the LMDZ model's performance in simulating cyclogenesis, cyclonic activity variability, and the associated processes spanning from the West African coasts to the tropical Atlantic basin. The study first delves into the model's ability to replicate West African cyclonic activity across the open Atlantic Ocean. Subsequently, it conducts a brief analysis of the mean conditions during the tropical Atlantic cyclone season, comparing periods of high and low cyclone activity to evaluate the model's proficiency in representing mean conditions and key aspects of the West African Monsoon (WAM). Finally, the study encompasses a space-time analysis of meteorological parameters linked to the progression of tropical cyclone Karl.

## EXPERIMENTAL

### Validation data

#### Reanalyses

Reanalysis involves merging data from various sources, including ground measurements, radiosondes, and satellite observations, with a weather forecasting model. The result is an extensive database of atmospheric and oceanic variables, covering global scales and ranging from short-term to long-term temporal resolutions. These datasets, known as reanalyses, offer a thorough and consistent representation of the earth's climate system (Dieng, 2015). We have chosen to validate the model against ERA-Interim reanalyses from the European Center for Medium-Range Weather Forecasts (ECMWF) for a period from 1979 to 2009. According to Dee et al. (2011), ERAI (ECMWF Re-Analysis Interim) is a frequently used global atmospheric reanalysis.

#### Observation

The NHC (National Hurricane Center) is the specialized institution responsible for monitoring and issuing warnings about cyclones in the North Atlantic and Eastern Pacific regions. At the conclusion of each cyclone season, the NHC compiles maps that contain detailed information about each cyclone. This information typically includes the cyclone's lifespan, date of formation, its position and intensity recorded at 6-h intervals, minimum pressure, maximum wind speed, and any associated material or human damage caused by the cyclone (Weinkle et al., 2018). These data sets from the NHC were utilized for a statistical study to analyse the temporal variability of cyclone activity. The study covered a period from 1979 to 2009 and focused on cyclone activity in the North Atlantic region.

### Tools

#### The LMDZ model

**Operating principle and basic discretized equations on the sphere:** LMDZ, specifically, is an atmospheric General Circulation Model (GCM) known for its substantial contribution to climate change projections featured in the reports of the IPCC (Hourdin et

al., 2006). It solves the primitive equations through its dynamic core module (Baek et al., 2014). Solving the basic equations of atmospheric dynamics involves a number of approximations and simplified versions for the study of atmospheric and even oceanic general circulation. These approximations primarily pertain to the thin-film approximation, which assumes that optical thickness is insignificantly small compared to the earth's radius, and the hydrostatic approximation.

1) Conservation of mass

$$\frac{D\rho}{Dt} + \rho \text{div}U = 0 \quad (1)$$

2) Conservation of potential temperature

$$\frac{D\theta}{Dt} = \frac{Q}{c_p} \left( \frac{P_0}{P} \right)^k \quad (2)$$

3) Conservation of momentum

$$\frac{DU}{Dt} + \frac{1}{\rho} - g + 2\Omega \wedge U = F \quad (3)$$

4) Conservation of secondary components

$$\frac{Dq}{Dt} = S_q \quad (4)$$

where  $U = u\vec{i} + v\vec{j} + w\vec{k}$  represents the three-dimensional wind vector (m/s),  $\rho$  the density of dry air ( $\text{kg/m}^3$ ),  $P$  the air pressure (Pa),  $g$  gravity ( $\text{m/s}^2$ ), and  $\Omega$  the angular velocity of the earth's rotation ( $\text{s}^{-1}$ ).

**The LMDZ5 "New physics":** LMDZ5 is the current version of the LMDZ atmospheric general circulation model (Hourdin et al., 2006) which is used for climate studies, climate change projections, and environmental studies. LMDZ5 is the atmospheric component of the IPSL Coupled Model (IPSL-CM5) used in particular for climate change projections in the frame of CMIP5. It introduces several improvements to its physics components, including a new boundary layer scheme that combines a turbulent diffusion model with a prognostic equation for turbulent kinetic energy, following approach. It also incorporates a "mass flow" scheme to represent coherent dry convective structures and cloud boundary layer structures described by Rio and Hourdin (2008). Furthermore, the model integrates a modified version of the Emanuel thunderstorm convection scheme, with changes in mixing probability prescriptions, closure mechanisms, and triggering criteria based on boundary layer characteristics, as outlined by Rio et al. (2009). The convection scheme is coupled with a parameterization addressing the formation of cold pockets from convective rain re-evaporation, influencing convection initiation and termination. These enhancements collectively refine the model's representation of complex atmospheric processes.

### Methods

In this research, the study focuses on identifying the environmental conditions conducive to cyclogenesis, the process of cyclone formation. To achieve this, horizontal sections of various atmospheric layers are analysed. This approach helps in pinpointing the essential requirements, including both dynamic and thermodynamic conditions that support the development of

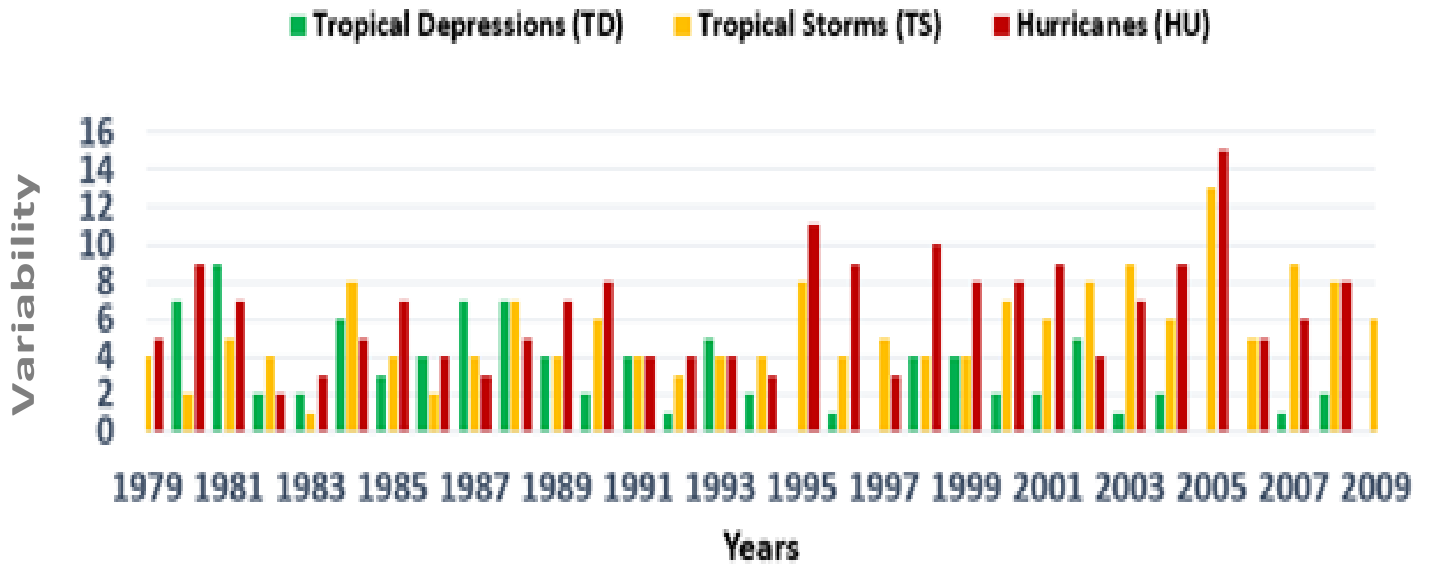


**Figure 1.** Interannual variability of cyclonic activity in the North Atlantic from 1979 to 2009.

cyclones. It also helps in identifying specific geographic regions and favorable time periods, such as July, August, and September (JAS), when cyclonic activity tends to be most prevalent.

The research begins with a statistical analysis of cyclone activity using data from the NHC archive. In this study, a tropical cyclone in the Atlantic basin is defined as an atmospheric disturbance that progresses through the stages of Tropical Depression (TD), Tropical Storm (TS), and hurricane (HU) in succession.

To assess cyclonic activity, we focus on the parameter "frequency," which refers to the annual count of TDs, TSs, and HUs observed from 1979 to 2009 (Figure 1). This approach allows for the identification of years with high activity years (HAY) and low activity years (LAY) in the Atlantic basin. These seasons are determined based on the interannual variability (Figure 1), where the average number of cyclonic activities and the standard deviation are calculated.

LAY are defined as those with a cyclonic activity count below  $\mu - \sigma$ , where  $\mu$  represents the average annual number of cyclonic activities calculated from 1979 to 2009, and  $\sigma$  is the associated standard deviation. In this context, LAY corresponds to the years 1982, 1983, 1987, 1994, 1997, and 2009. On the other hand, HAY are those with a cyclonic activity count exceeding  $\mu + \sigma$ . HAY in this study includes 1980, 1995, 1996, 1998, 2001, 2004, and 2005. These categorizations provide a basis for further analysis and investigation into the factors influencing cyclonic activity in the Atlantic basin.

The next step in the research involves conducting a composite analysis for the years of both high cyclonic activity (HAY) and low cyclonic activity (LAY) using the ERAI reanalysis dataset. The goal is to identify and understand the average seasonal patterns associated with these particular years. The comparison between the two average conditions of reanalysis and simulations will show us how well LMDZ captures the atmospheric conditions during these periods. Then, the 850 and 200 hPa relative vorticity and divergence are calculated from the ERAI wind data. These parameters are essential for understanding the dynamics and circulation patterns in the atmosphere during HAY and LAY years.

In the final phase of the research, a specific case study focuses on a synoptic-scale disturbance, particularly Hurricane Karl. The

objective is to conduct a detailed examination and comparison of this specific weather event. First of all, regarding this study case, a spatiotemporal tracking of hurricane Karl is done. This is accomplished by monitoring the minimum sea level pressure (SLP) associated with the system at 12 h intervals from September 16th to September 23rd. This tracking allows for a comprehensive understanding of the hurricane's movement and development over time.

The instantaneous speed of the disturbance and the average speed of translation were then calculated. To do this, the Haversine formula is used to calculate the distance between each two geographical points (longitude and latitude) on a sphere, such as the earth. This formula is particularly useful for determining distances on a sphere, such as the earth. It takes into account the curvature of the earth's surface when measuring distances between points. Here is the Haversine formula:

$$a = \sin^2\left(\frac{\Delta lat}{2}\right) + \cos(lat1) \times \cos(lat2) \times \sin^2\left(\frac{\Delta lon}{2}\right) \quad (5)$$

$$c = 2 \times \text{atan2}(\sqrt{a}, \sqrt{(1-a)}) \quad (6)$$

$$\text{distance} = R \times c \quad (7)$$

where  $\Delta lat$  is the difference in latitude between the two points,  $\Delta lon$  is the difference in longitude between the two points,  $lat1$  and  $lat2$  are the latitudes of the two points, respectively.  $R$  is the radius of the sphere (for example, the average radius of the earth in meters).

To provide a more comprehensive understanding of the spatiotemporal evolution of Hurricane Karl, several additional tools and techniques are utilized.

#### **Hovmöller diagram of relative vorticity (850 hPa)**

A Hovmöller diagram is created to visualize the spatiotemporal

evolution of relative vorticity at the 850 hPa level. This diagram is divided into two phases:

- 1) Zonal tracking (September 16 to 19th): Relative vorticity is averaged over latitudes between 10 and 20°N. This provides a zonal (East-West) perspective of the hurricane's behaviour during this period.
- 2) Meridional Tracking (September 20th to 23rd): Relative vorticity is averaged over longitudes between 50° and 45°W. This offers a meridional (North-South) view of the hurricane's characteristics during this phase.

#### **Daily anomalies of horizontal cross-section structures**

Daily anomalies are constructed to examine the horizontal cross-sectional structures associated with Hurricane Karl. These anomalies provide insights into how the hurricane's characteristics and structure change from its genesis, development to its dissipation. The analysis typically spans from the earth's surface to the upper troposphere, allowing for a comprehensive assessment of the hurricane's development. The data was processed, and the calculations were performed using Anaconda (Python) software in the Spyder environment.

## **RESULTS AND DISCUSSION**

### **Climatology of seasonal average conditions**

#### **On the surface (SLP and wind)**

Figure 2 shows the JAS seasonal mean of Sea Level Pressure (SLP, colours) and 10 m wind patterns (vectors) for ERA Interim (left) and LMDZ (right). In the ERA-Interim dataset (Figure 2a), the lowest SLP values are observed between the equator and latitude 14°N. This observation aligns with expectations, as this region corresponds to the Intertropical Convergence Zone (ITCZ), which typically extends from 8 to 17°N. The ITCZ is known as a key area where many tropical depressions originate (DeMaria et al., 2001). Around this latitude band, the north-easterly and south-westerly trade winds converge, as shown in Figure 2a. Figure 2b illustrates that, compare to ERAI, the LMDZ model captures the broad features of SLP and wind patterns during the JAS period but exhibits a slight overestimation of SLP intensity in certain regions, particularly in the Gulf of Guinea. The mean absolute error (MAE) between the model and observations indicates an error percentage of approximately 11%.

Anomalies associated with the season of high activity (HAY) and those of low activity (LAY) are presented in Figure 3. The HAY (LAY) is associated with a negative (positive) SLP anomaly in the north-western part of the Atlantic (Figure 3a and c). This area of lower SLP encompasses the north-western part of the MDR (Main Development Region), an area known for highly favorable meteorological conditions for cyclone formation. The wind

surface anomaly exhibits a cyclonic structure, centered on the area of lowest SLP in HAY (Figure 3a) and anticyclonic structure in LAY (Figure 3c).

These patterns are respectively consistent with the circulation expected during active cyclone and less active cyclone seasons. The model successfully reproduces these observed anomalies associated with HAY and LAY.

However, it is noted that the model tends to overestimate the SLP anomalies in the Gulf of Guinea region. Overall, these findings indicate that the model captures the essential features of SLP and wind patterns during high and low cyclonic activity years, providing valuable insights into the atmospheric dynamics associated with different cyclone seasons.

#### **In the lower troposphere (850 hPa - relative vorticity and wind)**

Figure 4 shows the climatology at 850 hPa of the relative vorticity ( $s^{-1}$ , in colour) and the horizontal wind patterns ( $m \cdot s^{-1}$ , in vector) and the anomalies associated with seasons of high and low cyclonic activity (Figure 5).

On the continent, a positive relative vorticity is located on either side of the 15°N latitude (Figure 4a). According to Diedhiou et al. (2001) and Fink and Reiner (2003), these structures correspond to the trajectories of African Easterly Waves (AEW) propagating north and south of the African Easterly Jet (AEJ). The southern AEWs, deriving energy from the AEJ, are located in the humid zone and play a role in modulating rainfall in West Africa (Pytharoulis and Thorncroft, 1999; Chen, 2006). The northern AEWs are favored by baroclinic energy conversions (Burpee, 1972; Diedhiou et al., 1999). The two wave paths merge over the Atlantic Ocean, in the ITCZ, where most tropical depressions also originate (Figure 4a). Indeed, a positive vorticity is a necessary parameter for cyclogenesis in the basin. Winds converge toward the ITCZ, slowing down over land due to friction. The LMDZ model simulates the spatial distribution of vorticity fields, highlighting the trajectories of southern and northern AEWs. However, it tends to underestimate the vorticity intensity in the ITCZ and along both AEW paths (Figure 1b). The mean absolute error (MAE) between the observed and model vorticity fields is approximately 12%.

In HAY, positive vorticity anomalies are observed in the western oceanic zone, above 15°N and 30°W, accompanied by cyclonic wind circulation (Figure 5a). Over the continent, positive vorticity anomalies reflect the activity of northern AEWs north of the AEJ, with a cyclonic circulation in the Saharan Air Layer (SAL). However, negative vorticity is noted in the same area during LAY (Figure 5c) with an anticyclonic wind circulation. Thus, the southern AEWs are more active during LAY, indicating the enhanced activity of southern

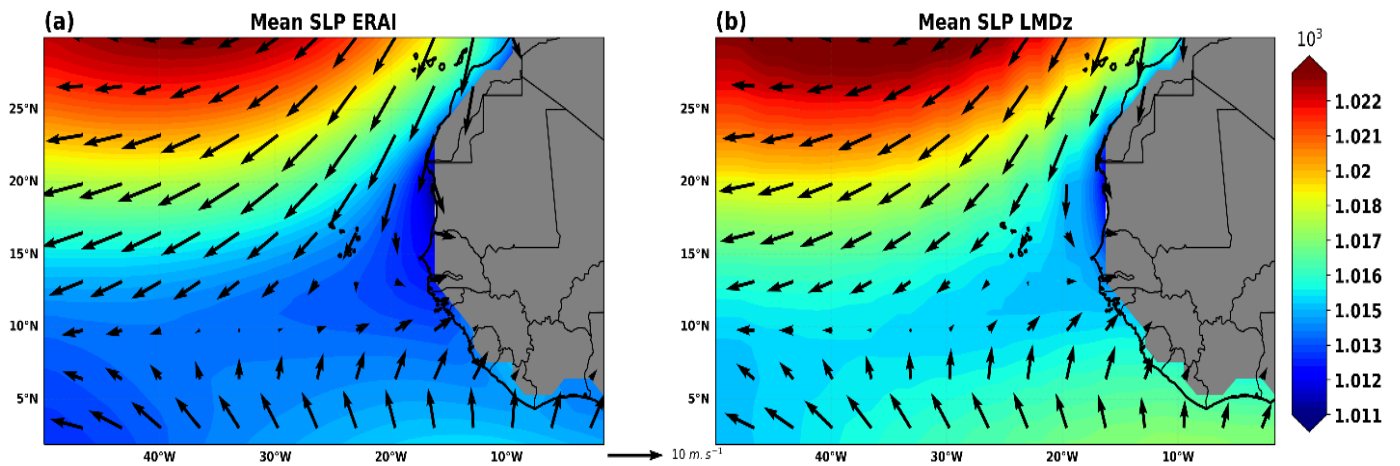


Figure 2. Seasonal average (July-September from 1979 to 2009) of SLP (hPa, in colour) and average horizontal wind at 10 m ( $m \cdot s^{-1}$ , in vector) for ERA Interim (a) and LMDZ model (b).

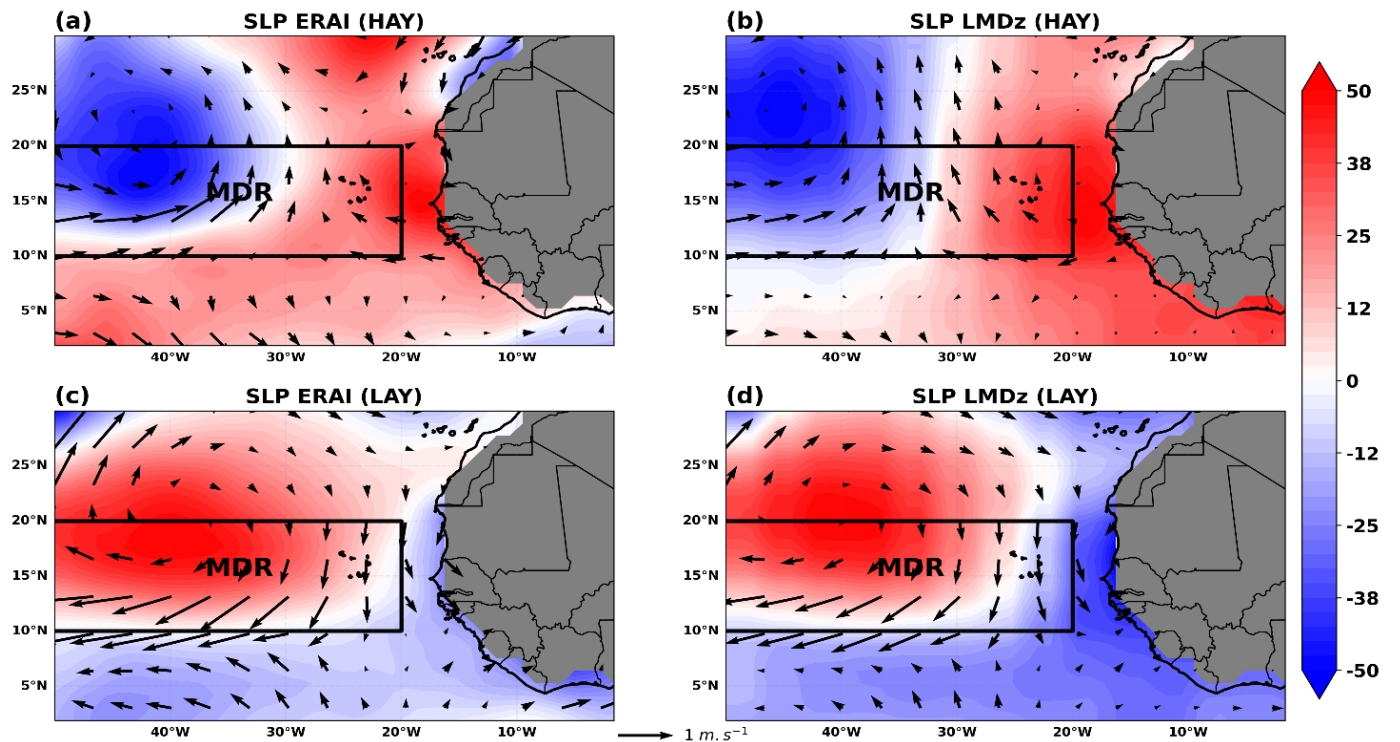
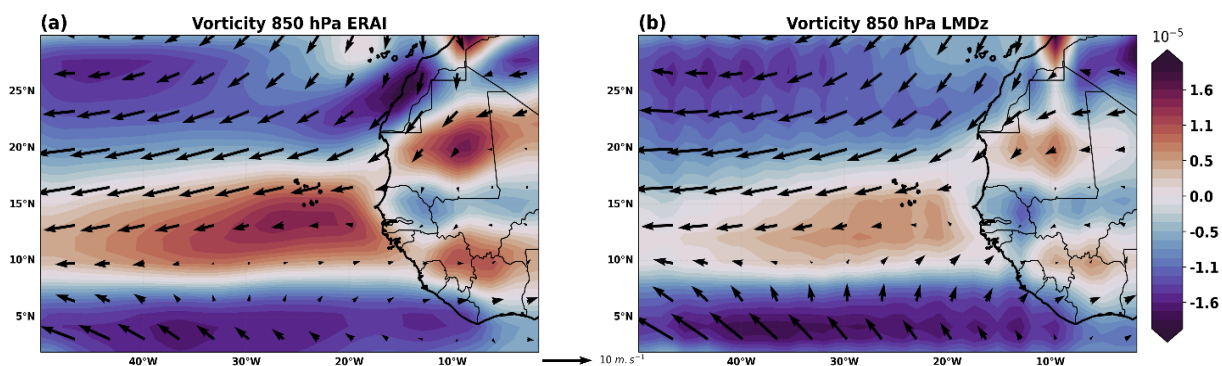


Figure 3. Seasonal anomalies of SLP ( $10^{-2} hPa$ , in colour) and horizontal wind ( $m \cdot s^{-1}$ , in vector) for HAY (top) and LAY (bottom) for ERA Interim (a, c) and LMDZ (b, d).

AEWs. The model reproduces these patterns, including the distribution of relative vorticity anomalies and AEW activity in HAY and LAY (Figure 2d). Similarly, the model replicates the trends in the wind field anomalies at 850 hPa.

***In the mid-troposphere (700 hPa - relative humidity and wind)***

Globally, areas with high humidity ( $>70\%$ ) in the seasonal averages are concentrated between the equator and



**Figure 4.** Seasonal average (July-September from 1979 to 2009) of relative vorticity ( $s^{-1}$ , in colour) and average horizontal wind ( $m. s^{-1}$ , in vector) at 850 hPa for ERA Interim (a) and LMDZ model (b).

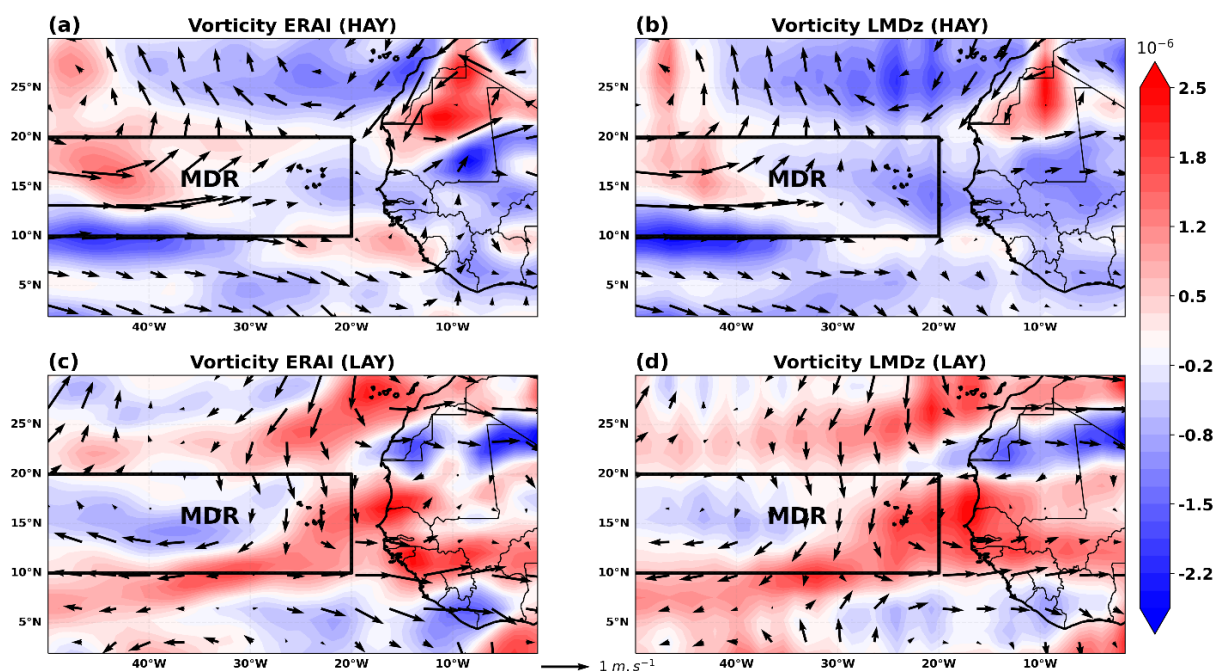


**Figure 5.** Seasonal anomalies of relative vorticity ( $s^{-1}$ , in colour) and horizontal wind ( $m. s^{-1}$ , in vector) at 850 hPa for HAY (top) and LAY (bottom) for ERA Interim (a, c) and LMDZ (b, d).

14°N (Figure 6a), corresponding to the ITCZ area. The circulation at 700 hPa is influenced by the African Easterly Jet (AEJ), with its maximum speed typically between 12°N and 18°N varying around 12  $m.s^{-1}$ . Maxima in relative humidity were observed just south of the AEJ. The LMDZ model is capable of representing the seasonal average of relative humidity (Figure 6b), which closely resembles the ERA-Interim reanalysis data. However, the model tends to overestimate relative humidity, particularly in the 5 to 10°N latitude band. The mean absolute error (MAE) between observations and the model indicates a

14% error in relative humidity at 700 hPa.

A positive anomaly was found (Figure 7a) in the zone covering the entire MDR area during HAY. Thus, this moisture is crucial at this level and is synonymous with high-water content that helps resist downdrafts. In addition, a wind anomaly with a cyclonic circulation is noted in the positive relative humidity anomaly area. The southerly winds are accelerated with a slowing of the AEJ off the basin as well as acceleration to the East of the basin. In contrast to the HAY, LAY is associated with a negative anomaly (Figure 7c) in relative humidity, with an

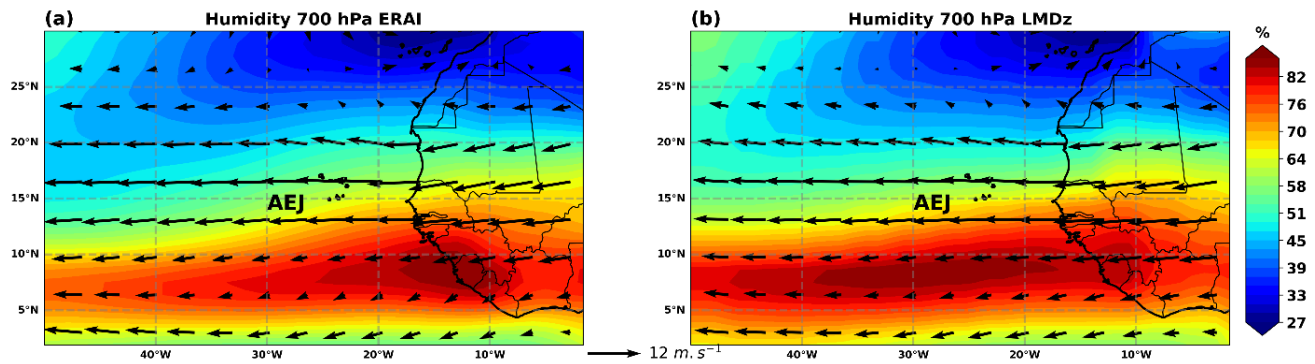


**Figure 6.** Seasonal average (July-September from 1979 to 2009) of relative humidity (% , in colour) and average horizontal wind ( $m. s^{-1}$ , in vector) at 700 hPa for ERA Interim (a) and LMDZ model (b).

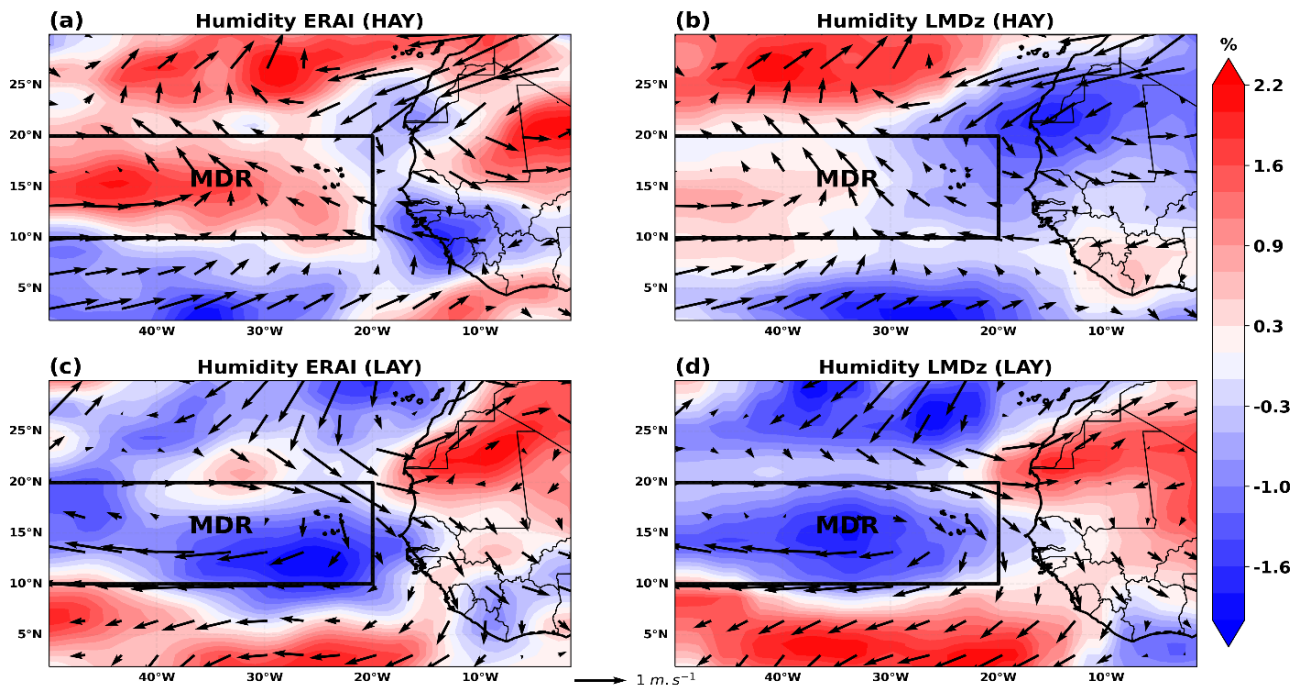


**Figure 7.** Seasonal anomalies of relative humidity (% , in colour) and horizontal wind ( $m. s^{-1}$ , in vector) at 700 hPa for HAY (top) and LAY (bottom) for ERA Interim (a, c) and LMDZ (b, d).

anticyclonic circulation of winds. These conditions are synonymous with a drying of the middle troposphere, which favours downward movements that are not conducive to maintaining the disturbance. Wind patterns in LAY show behaviour opposite to that of HAY.

The findings emphasize the importance of relative humidity in the middle troposphere as a critical factor for cyclone genesis in the tropical Atlantic. The LMDZ model successfully reproduces the different relative humidity structures in the basin during HAY and LAY, while capturing the behaviour of the AEJ for each season.

***In the upper troposphere (200 hPa - divergence and wind)***

The analysis of the atmosphere at the 200 hPa level, which includes features like the Tropical Easterly Jet (TEJ, with wind speeds around 16 m/s) and Subtropical Westerly Jet (JOST, with wind speeds around 18 m/s), provides valuable insights into the West African Monsoon (WAM) and its relationship with cyclonic activity. These opposing zonal flows exist between 5-10°N and 24-30°N, respectively (Figure 8a). The ERAI reanalyses exhibit a

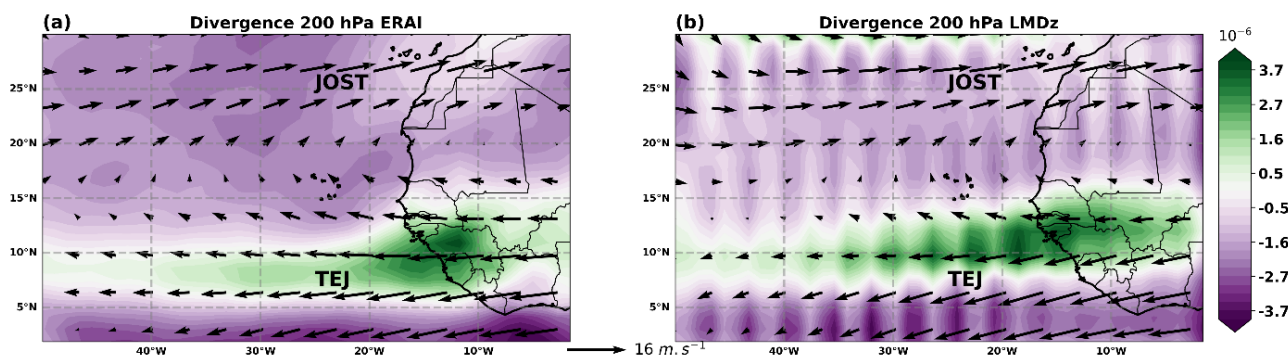


**Figure 8.** Seasonal average (July-September from 1979 to 2009) of divergence ( $s^{-1}$ , in colour) and average horizontal wind ( $m \cdot s^{-1}$ , in vector) at 200 hPa for ERA Interim (a) and LMDZ model (b).

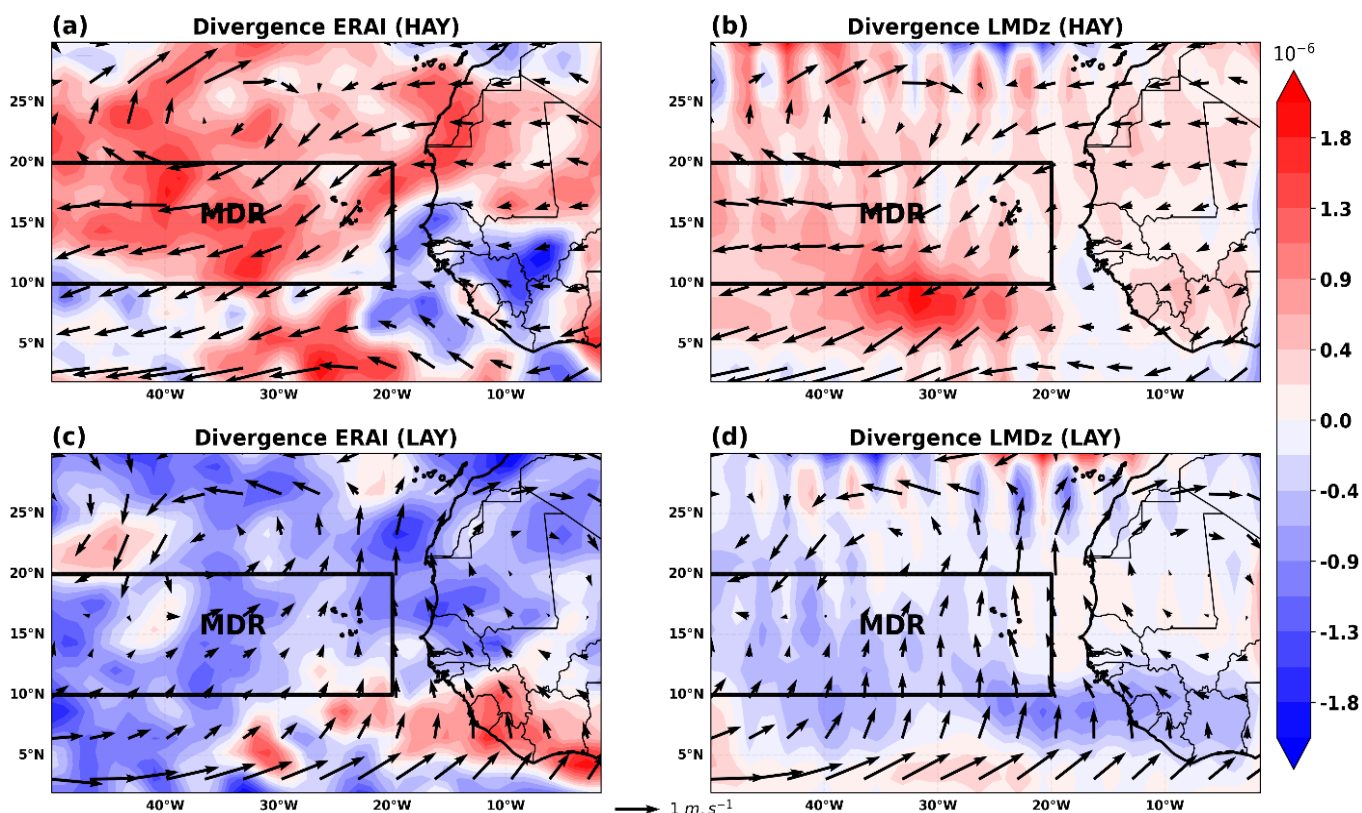


**Figure 9.** Seasonal anomalies of divergence ( $s^{-1}$ , in colour) and horizontal wind ( $m \cdot s^{-1}$ , in vector) at 200 hPa for HAY (top) and LAY (bottom) for ERA Interim (a, c) and LMDZ (b, d).

significant divergence above the ITCZ band, area of maximum relative vorticity and humidity in the low and medium layer (Figures 4a and 6a) and the lowest SLP (Figure 2a). Indeed, the divergence at 200 hPa is essential for the maintenance of the disturbances as it supports the evacuated ascending flows from the surface, thus confirming the results of Chen (2006). The

model is able to reproduce the wind field's structure, with intensity similar to the reanalyses and a good spatial distribution of the divergence field in the seasonal mean with a MAE of 17%. However, the model slightly overestimates the seasonal divergence field, especially in the vicinity of the ITCZ band.

HAY is associated with a positive divergence anomaly

and an anticyclonic wind circulation anomaly over the Azores High Pressure (Figure 9a). In contrast to HAY, LAY shows a negative divergence anomaly accompanied by a cyclonic circulation anomaly (Figure 9c). Intense seasons are associated with a weak strengthening of the TEJ while it is strongly slowed down during low activity seasons. This result confirms the work of Camara (2006) who showed that AEWs that develop into tropical cyclones in the Atlantic evolve in an environment with strong TEJ. The LMDZ model successfully reproduces the observed anomaly trends in divergence and wind patterns during HAY and LAY, providing further evidence of the relationship between the West African Monsoon, jet streams, and cyclonic activity in the tropical Atlantic.

In term of the dynamic point on AEWs structures, small differences between the HAY and LAY are noted in the relative vorticity anomaly. This would imply that wave activity plays a minor role in controlling the seasonal variability of cyclogenesis in the tropical Atlantic. However, over the continent, the AEWs north of the AEJ appear to be more active during the HAY. During HAY, it was observed that:

- 1) A slowdown of the AEJ, especially offshore, associated with a convergence anomaly in the middle layers.
- 2) A strong acceleration of the TEJ associated with a strong divergence anomaly in the higher layers of the atmosphere.

The combination of the mid-layer convergence anomaly and the high-layer divergence anomaly supports deep convection by strengthening the updrafts. In contrast to the HAY, the LAY are mainly marked by:

- 1) AEJ acceleration associated with high AEWs activity at 850 hPa.
- 2) A slowdown of the TEJ associated with a convergence anomaly at 200 hPa.

Here again, the combination of mid-layer relative humidity and divergence anomalies at 200 hPa inhibits convection by favouring subsidence.

Overall, these first results on the seasonal conditions of cyclonic activity in the tropical Atlantic show a good spatial coincidence between the reanalysed and simulated fields. Consequently, the model concedes the ability to represent cyclonic parameters on a climatological scale as well as certain characteristics of the monsoon with more accurate results at the surface than in the upper troposphere. Nevertheless, the model exhibits minor biases in the intensity of the SLP fields, relative vorticity, humidity, and divergence. These discrepancies might be attributed to the parameterization of the model's new version, where the convection scheme is linked to the parameterization of cold pockets formed beneath thunderstorms due to the re-evaporation

of convective rainfall, as described by Sane (2011).

Furthermore, several biases are noticeable in the Gulf of Guinea region, which can be attributed to the model's underestimation of low clouds, as indicated by Hourdin et al. (2006), and the fact that this region is prone to convection.

## Special case of Atlantic cyclone

### *Tracks of tropical disturbance associated with Karl*

Figure 10 displays the tracks of the tropical disturbance associated with Hurricane Karl from September 16th to 23rd, 2004, in the tropical North Atlantic.

The observations show a translation speed averaging  $2.74 \text{ m.s}^{-1}$  (Figure 10) from September 16 to 19th. In the simulation, the mean translation speed is  $3.05 \text{ m.s}^{-1}$  with an instantaneous speed higher than NHC and closer to ERAI (Table 1). In fact, during this period, the model's translation speed is faster than the observations by more than  $0.31 \text{ m.s}^{-1}$ . In other words, for every 100 m traveled by the disturbance in the observations, the model adds 5 m. However, the speed difference between ERAI and LMDZ becomes higher during the track from September 19th to 23rd. During this period, the disturbance slows down to less  $0.54 \text{ m.s}^{-1}$  in the observations. So, the model reproduces the slowing down of the system during this period, but with less deceleration ( $0.15 \text{ m.s}^{-1}$ ) than observed. This deceleration of the hurricane-strengthened system may suggest that the intensification of the disturbance fields is causing them to slow down. The trend aligns with a study by Lorck (2019), which showed that as Hurricane Dorian intensified and approached the Bahamas, its forward motion slowed considerably, to less than  $0.5 \text{ m.s}^{-1}$ .

### *Translation speed*

Figures 11 and 12 depict Hovmöller diagrams of the vorticity at 850 hPa, illustrating the westward and northward movement of Hurricane Karl from September 16 to 19th and then from September 20th to 23rd, respectively.

The Hovmöller diagram of the vorticity at 850 hPa shows a disturbance moving westward since its genesis. The tropical depression originated on September 16th near the Cape Verde Islands and developed into a tropical storm the following day. It continued to move westward and intensified into a hurricane on September 18th (Figure 10). The system further evolved and started to move northwards, strengthening into a category 3 major hurricane between September 19 and 20th (Figure 11). It remained a major hurricane, reaching category 4 on the next day. The disturbance maintained its intensity

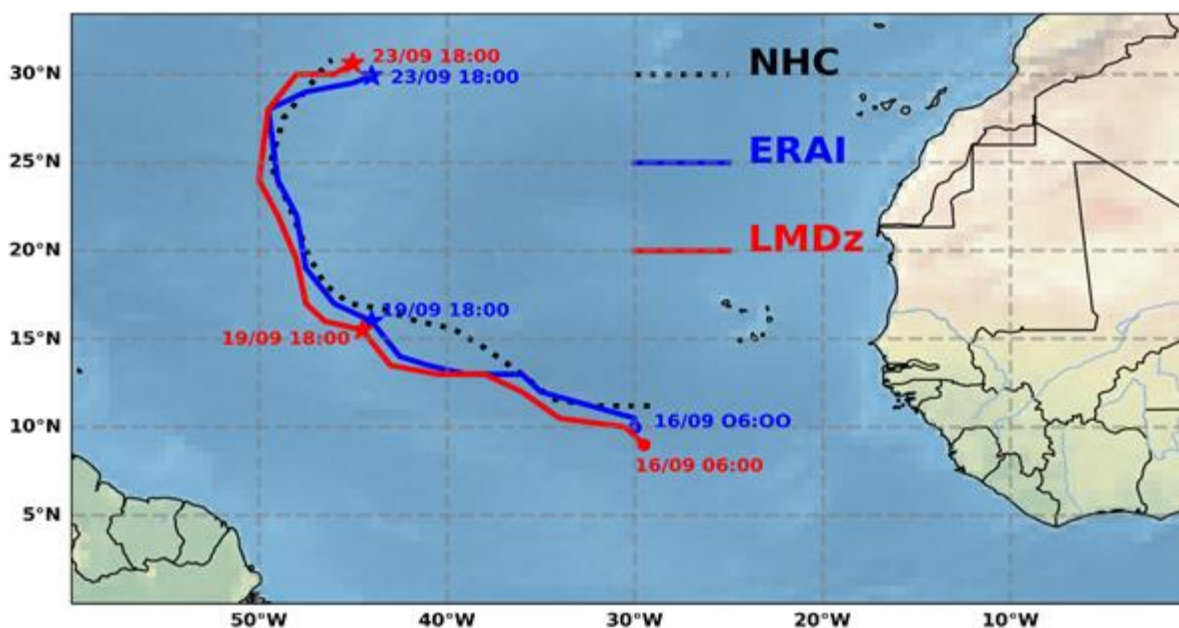


**Figure 10.** Observed and simulated track at 12h interval of Hurricane Karl from 16th to 23rd September 2004. The dotted line represents the NHC trajectory, ERAI the black line, and LMDz the red line.

**Table 1.** Instantaneous speed at genesis's place (29°W, 11°N) and translation mean speed in  $m.s^{-1}$ .

Variable	NHC	ERA Interim	LMDz
Instantaneous speed at genesis's place	1.02	1.28	3.61
Translation mean speed from September 16 to 19th	2.18	2.74	3.05
Translation mean speed from September 19th to 23rd	2.08	2.20	2.90

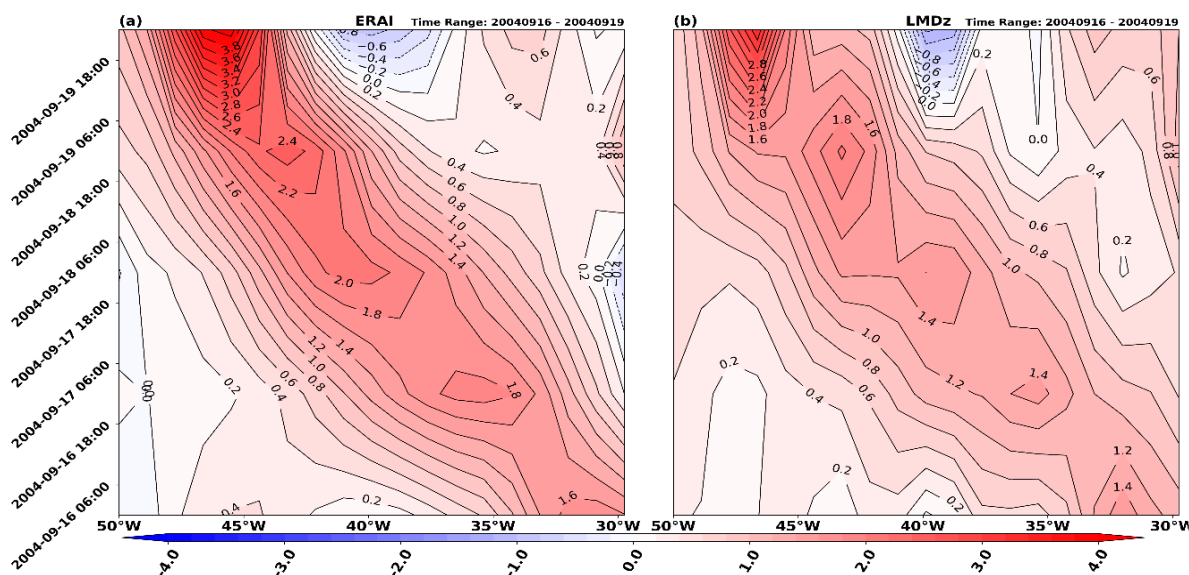


**Figure 11.** Hovmöller diagram of the vorticity at 850 hPa of ERAI (a) and LMDz (b) from 16<sup>th</sup> to 19<sup>th</sup> September at 12h interval averaged at 10 – 20° N latitudes.

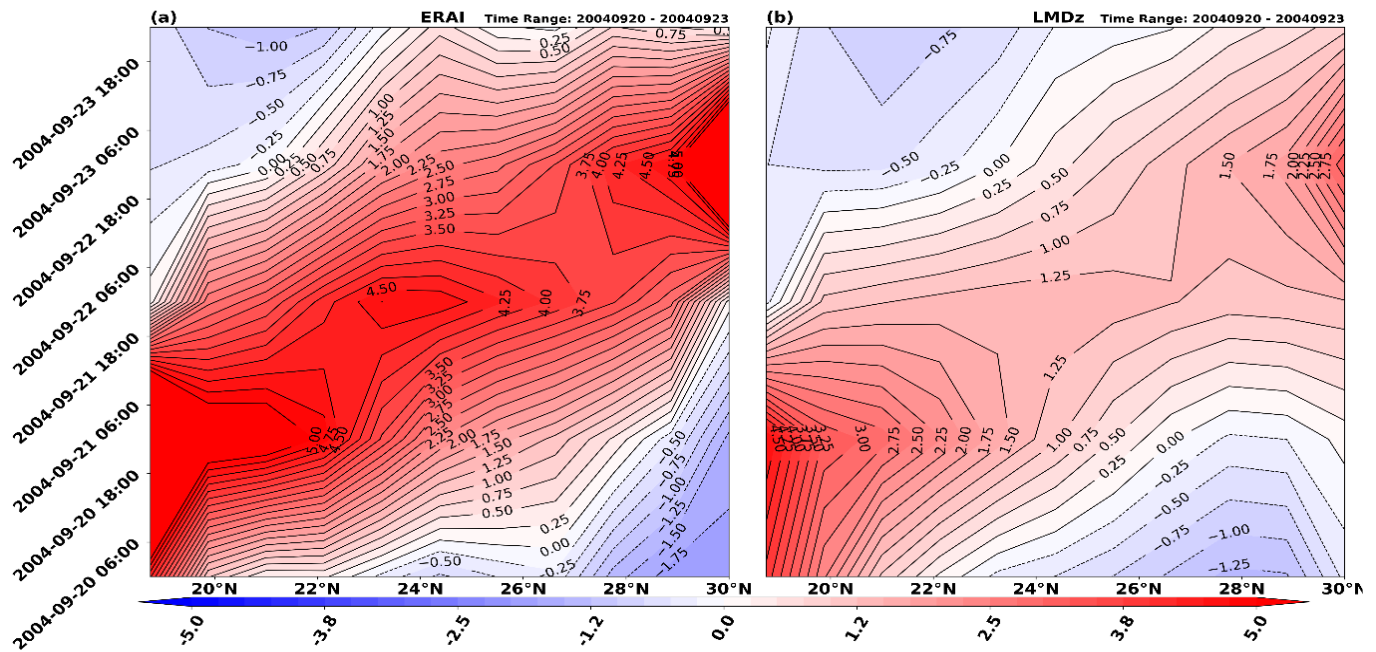


**Figure 12.** Hovmöller diagram of the vorticity at 850 hPa of ERA1 (a) and LMDz (b) from 20<sup>th</sup> to 23<sup>th</sup> September at 12h interval averaged at 50 – 45° W longitudes.

from September 22nd to 23rd and reached a position of 27° North before dissipating on September 24th. Importantly, Hurricane Karl did not pose a threat to any inhabited land. It followed a trajectory toward the northwest and then north, aligning with the results of Beven (2004). The model successfully reproduces the different trajectories of the disturbance as well as the differences in the relative vorticity fields for the various categories of the hurricane.

**Evolution of horizontal cross-section structures**

**On the surface**

Figure 13 displays daily anomalies of sea-level pressure (SLP) and surface wind from September 15 to 20th, 2004, showing the evolution of Hurricane Karl.

On the eve of the genesis of the disturbance (September 15th), a vortex circulation progressively sets up toward 10°N, 25°W (Figure 13\*), which are pre-existing conditions for the genesis of Hurricane Karl (born towards 11°N 29°W). On September 16th, the system was born as a Tropical Depression (TD) and evolved with an increasingly intense and more pronounced cyclonic circulation surrounding a lower SLP. By September 17th, the system had a fairly large negative SLP anomaly and evolved toward the northwest (Figure 13TS), reaching the stage of a Tropical Storm (TS). On the subsequent day (18/09), the disturbance underwent intensification and

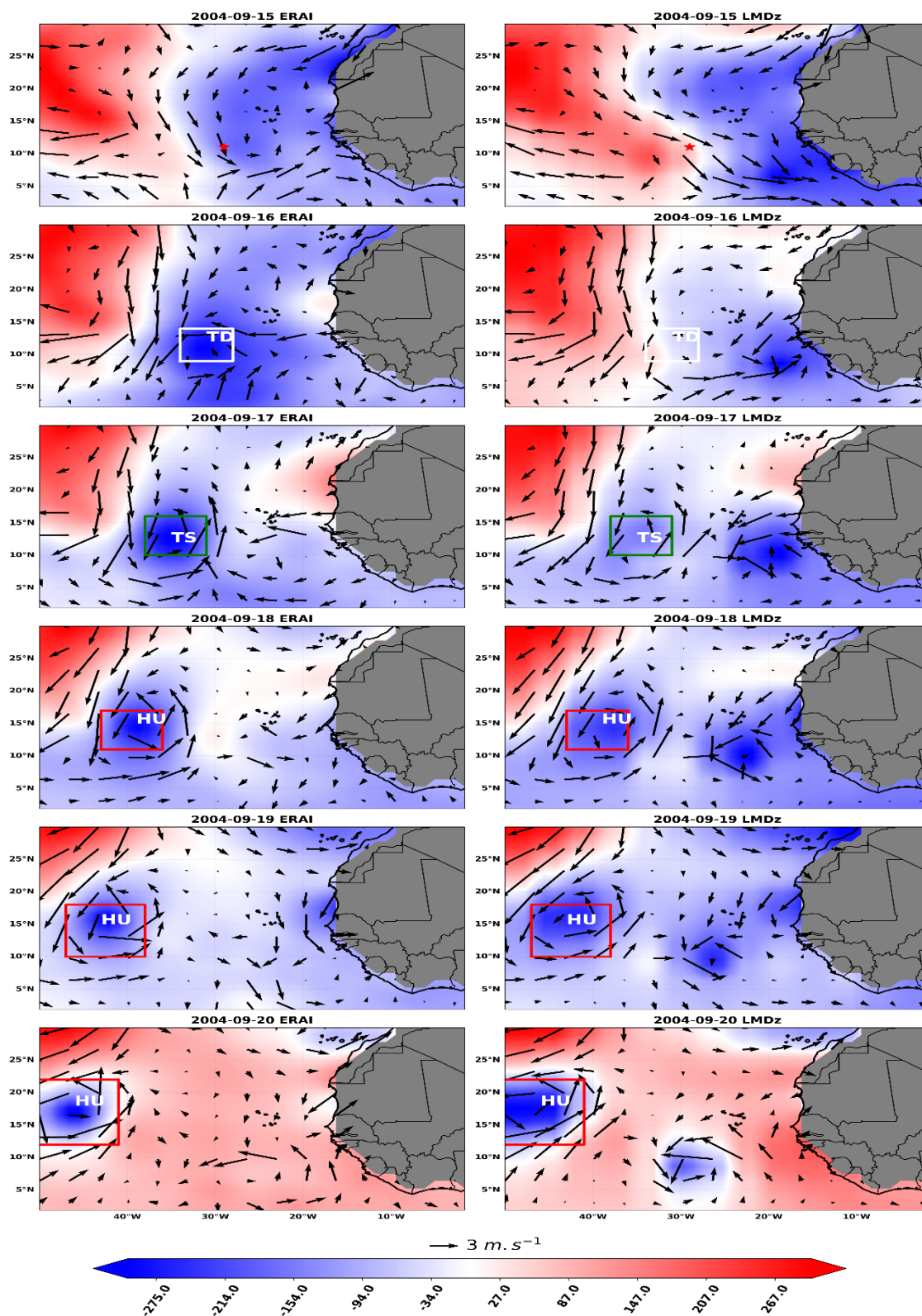
evolved into a hurricane, exhibiting more distinct cyclonic wind circulation patterns and a negative SLP anomaly (Figure 13HU). Thereafter, it evolves by remaining in the HU stage until it dissipates from the tropics on September 24th. In the simulation, on September 15th, LMDz does not show signs of pre-existing conditions at Karl's birthplace (11°N, 29°W).

The SLP anomaly becomes negative in the simulation, unlike ERA1, and a cyclonic wind circulation begins to form (TD). However, these conditions are a little late to set up compared to those of ERA1 where they are more structured at this stage. At the TS stage, the system is still less intense and less developed in terms of wind circulation and SLP anomaly. However, it catches up with a similar representation the next day (HU) when it has strengthened to hurricane status. At the HU stage on September 18, 19 and 20th, the model shows a low SLP anomaly and a well closed cyclonic wind circulation at the surface. The simulation successfully replicates the evolution of Hurricane Karl, with some variations in the early stages compared to the reanalysis but a strong resemblance as the hurricane intensifies.

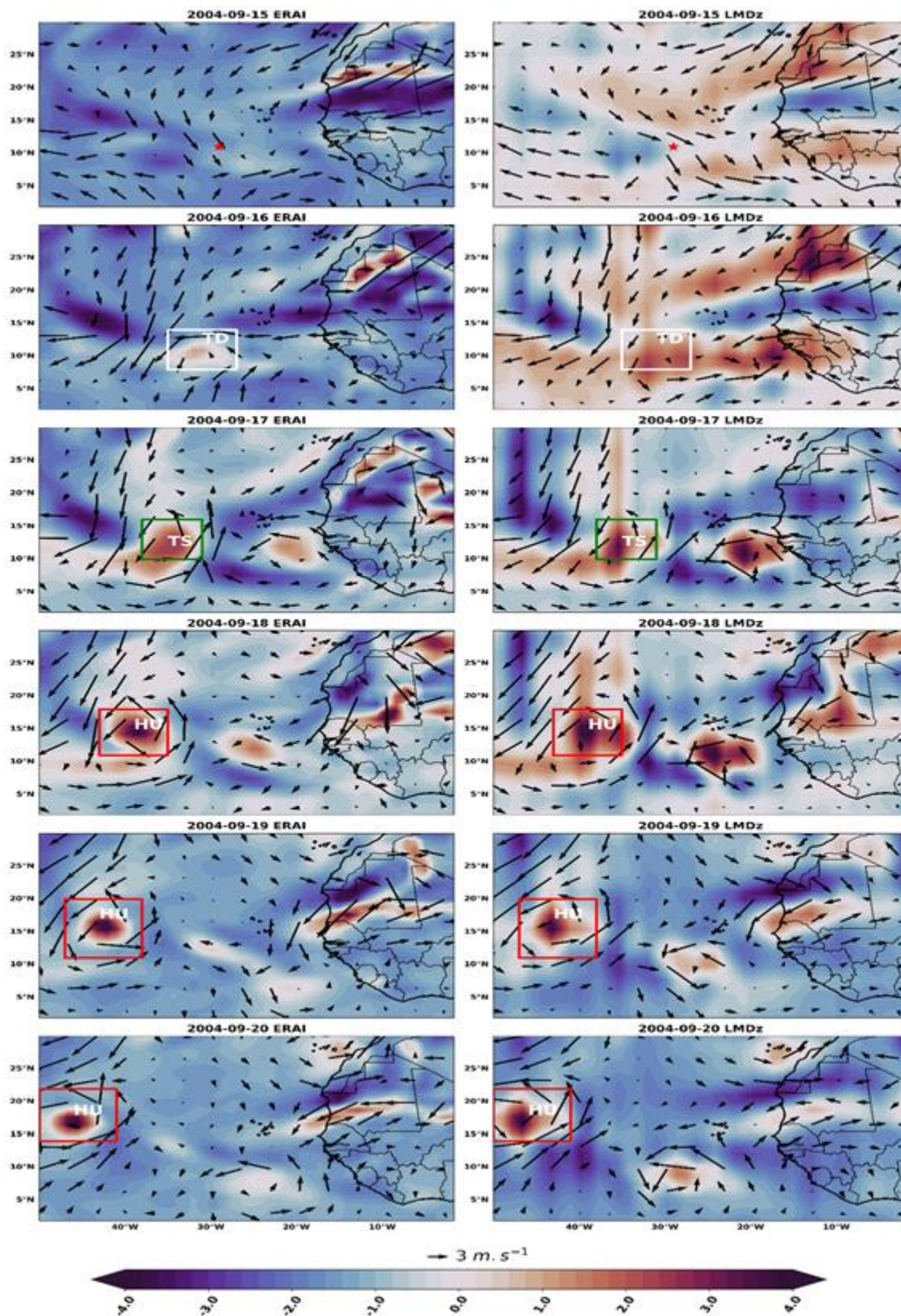
**In the lower troposphere**

Figure 14 illustrates the horizontal sections of daily relative vorticity and horizontal wind anomalies at 925 hPa from September 15 to 20th, 2004.

On the eve of the system's development, the relative



**Figure 13.** Horizontal cross-sections of daily SLP anomalies (hPa, in colour) and horizontal 10 m wind anomalies ( $m \cdot s^{-1}$ , in vectors) of ERAI and LMDZ from 15th to 20th September 2004. The red star represents Karl's birthplace. The white, green and red rectangles represent the system at the stage of Tropical Depression (TD), Tropical Storm (TS) and Hurricane (HU), respectively.



**Figure 14.** Horizontal cross-sections of daily relative vorticity anomalies ( $10^{-5} \text{ s}^{-1}$ , in colour) and horizontal wind ( $\text{m} \cdot \text{s}^{-1}$ , in vectors) at 925 hPa analysed by ERAI and LMDZ from 15 to 20th September 2004.

vorticity anomaly field in ERAI is negative over most of the basin but shows strengthening southerly winds. This latter is a crucial factor for the cyclonic circulation's development. On September 16th (TD), the reanalysed field exhibits a well-developed cyclonic circulation with a positive vorticity anomaly around 10°N to 30°W. The circulation winds around the system gradually intensify, and becoming more increasingly important during the TS stage (Figure 14TS). The system strengthens into a hurricane on September 18th as it moves north-westward (Figure 14HU) with more representative dynamic structure fields throughout its HU stage. In the model, a positive vorticity anomaly is observed one day before the system's genesis, but the wind anomaly is less structured compared to ERAI on the day of the depression's birth (TD). The delay observed in detecting the TD stage at the surface is not visible at 925 hPa relative vorticity in the model. From the tropical storm (TS) stage onwards, the model successfully replicates the dynamic structures of the system similar to ERAI, although it slightly overestimates the relative vorticity. As the system strengthens into a hurricane on September 18th (HU), LMDZ reproduces it similarly to ERAI. These results indicate that LMDZ provides a reasonable representation of the relative vorticity and dynamic structures of Hurricane Karl, although there are some differences in the early stages of the system's development.

### ***In the mid-troposphere***

Figure 15 presents the horizontal sections of daily relative humidity and horizontal wind anomalies at 700 hPa from September 15 to 20th, 2004.

On September 15th, the daily relative humidity anomaly is around 6%(\*), and it becomes increasingly wet on September 16th (TD) and 17th (TS) with a more pronounced structure. The horizontal wind vortex circulation progressively sets up during these two days in the TD and TS phase. During the intensification into hurricane (HU), the reanalysis shows a system evolving towards the northwest with well-developed winds. The latter bring more moisture and sustain the cyclonic circulation confirming Beven (2004) to the intensification of the disturbance to category 4. LMDZ exhibits a negative daily relative humidity anomaly at the system's birthplace (\*). However, on the genesis day (TD), the daily relative humidity anomaly becomes positive in the simulation. At 700 hPa, LMDZ struggles to reproduce the system in the TD and TS phases, as previously observed at the surface. On September 18th, when the system strengthens into a hurricane (HU), an intense eddy circulation becomes more evident. From this point onward, similar to ERAI, LMDZ reproduces the daily relative humidity and wind anomalies with a more structured system. The results suggest that LMDZ has

difficulty in capturing the early stages of the system's development, particularly in the TD and TS phases.

However, it gradually improves its representation of the system, aligning more closely with ERAI as the system intensifies into a hurricane.

### ***In the upper troposphere***

Figure 16 presents the horizontal sections of divergence and horizontal wind anomalies at the 200 hPa level, analyzed by ERAI and simulated by LMDZ from September 15 to 20th, 2004.

On the system's genesis day, ERAI exhibits a divergence intensifying at (10°N to 33°W) with an increasingly significant anticyclonic circulation (TD). On September 17th, when the system strengthens into a tropical storm (TS), ERAI shows a larger divergence anomaly at 200 hPa, which supports deep convection by strengthening the updrafts. As the system evolves into a hurricane (HU), the reanalysis indicates a more substantial divergence anomaly and an anticyclonic circulation. In contrast to ERAI, the simulated divergence anomaly on September 15th remains negative at Karl's genesis location (11°N, 33°W). The model struggles to represent systems with less developed intensity in all layers above. In contrast to ERAI, the simulated divergence anomaly on September 15th remains negative at Karl's genesis location (11°N, 33°W). The model struggles to represent systems with less developed intensity in all layers above. As the system strengthens into a tropical storm (TS) and then into a hurricane (HU), LMDZ provides a more representative simulation, but the divergence anomaly remains less pronounced than in the reanalysis. The results suggest that LMDZ is still unable to capture the early stages of the system's development and has difficulty representing the divergence anomalies seen in ERAI. While it gradually improves its representation of the system as it intensifies, the model's divergence anomalies are generally weaker than those observed in the reanalysis.

The second part of the results, which focuses on synoptic scales, provides insights into the LMDZ climate model's ability to replicate meteorological parameters associated with tropical disturbances. The model demonstrates success in terms of temporal and spatial analysis, as well as tracking a trajectory that is closely aligned with the ERAI reanalysis. These findings indicate that the LMDZ model can effectively reproduce cyclonic structures both in terms of timing and spatial distribution. However, a notable observation from this analysis is the model's delay in detecting the Tropical Depression (TD) stage, which is the initial phase of tropical cyclone development. This suggests that the model may have limitations in representing the early stages of tropical cyclone formation.

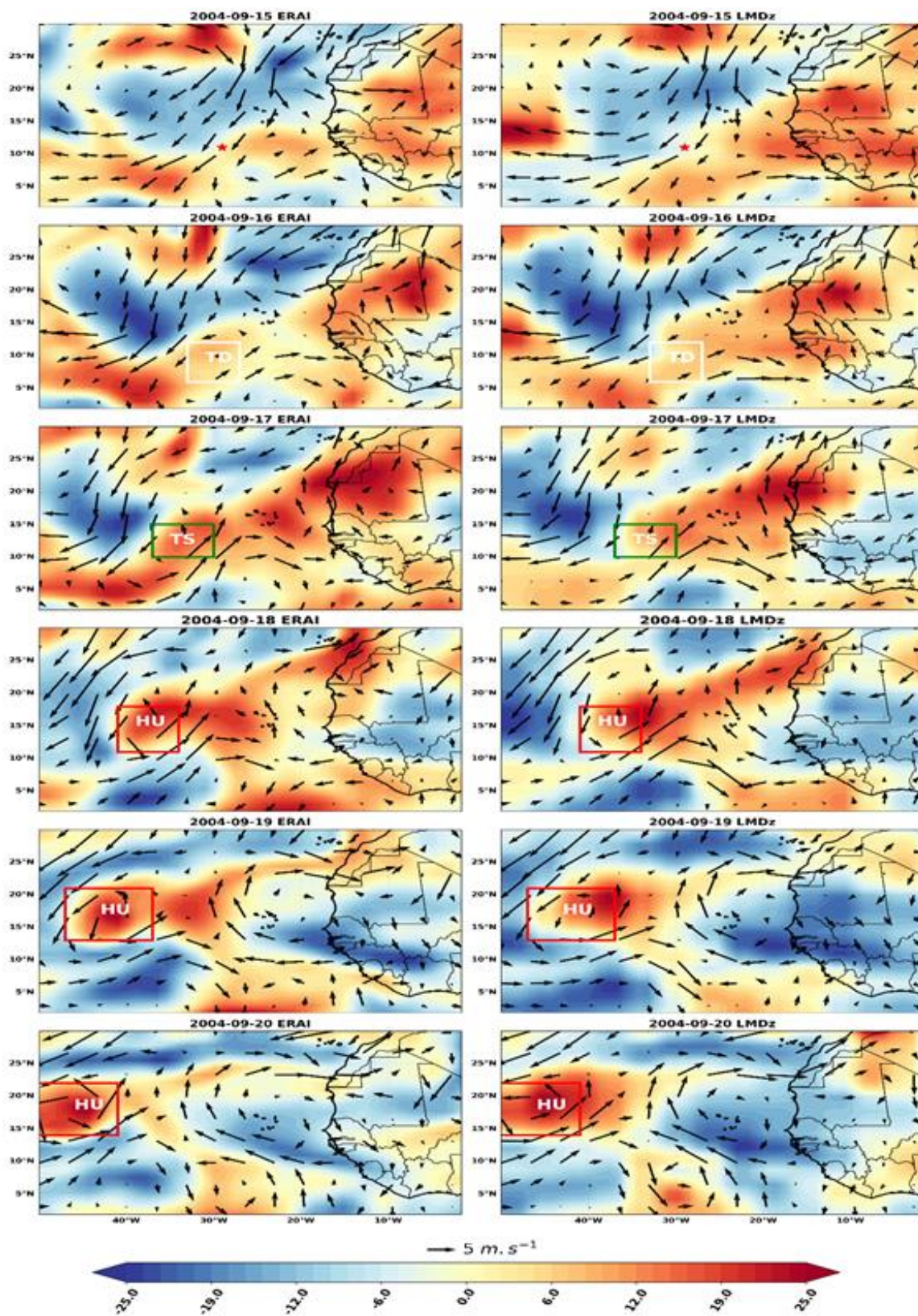


**Figure 15.** Horizontal cross-sections of daily anomalies of relative humidity (% in colour) and horizontal wind ( $m \cdot s^{-1}$ , in vectors) at 700 hPa analysed by ERAI and LMDz from 15 to 20th September 2004.

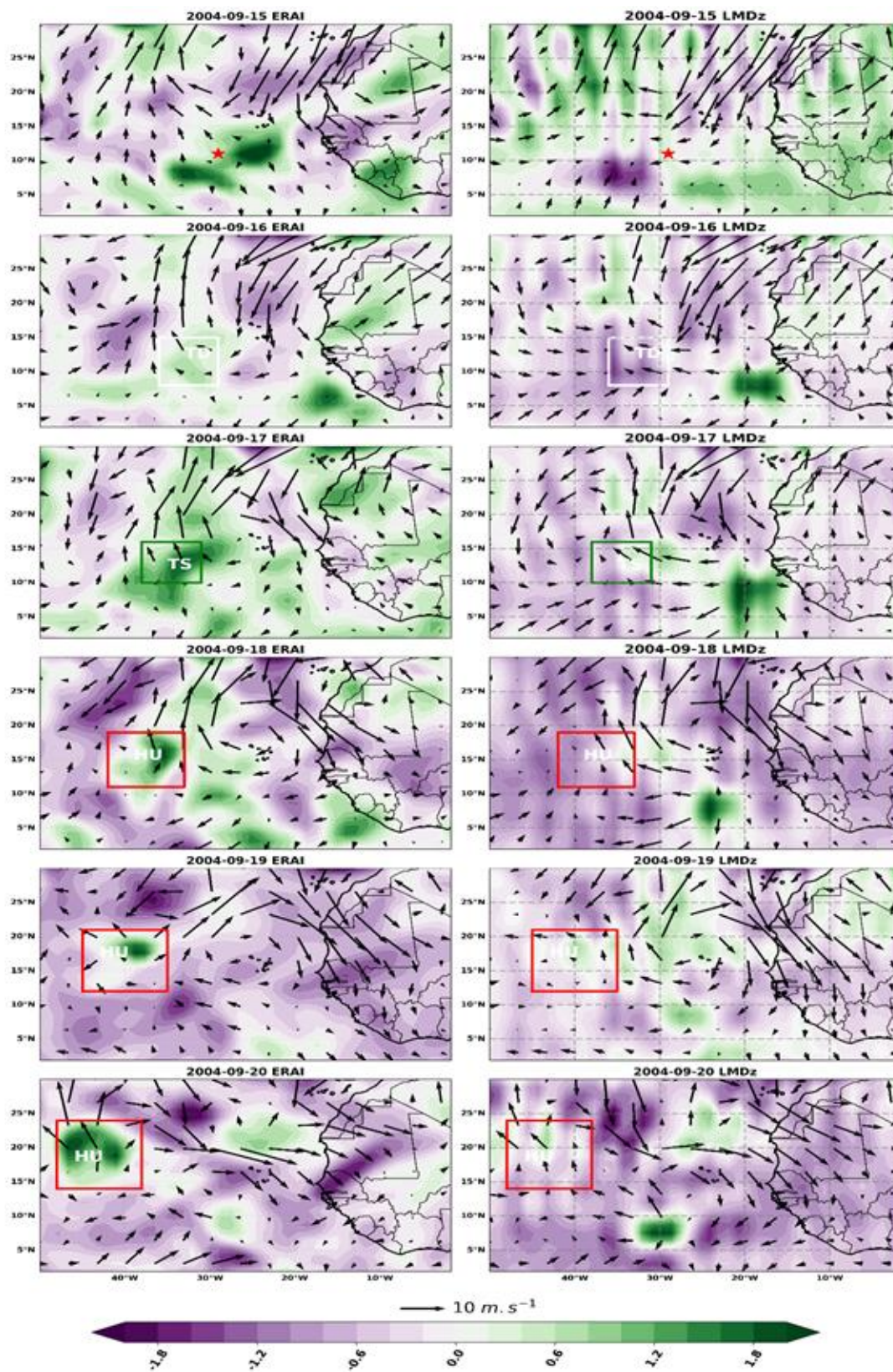


**Figure 16.** Horizontal cross-sections of daily divergence ( $10^{-5} \text{ s}^{-1}$ , in colour) and horizontal wind ( $\text{m s}^{-1}$ , in vectors) anomalies at 200 hPa analysed by ERAI and LMDZ from 15 to 20th September 2004.

## CONCLUSION AND PERSPECTIVES

This study aimed to assess the LMDZ model's ability to reproduce cyclogenesis processes and the associated environmental conditions through both interannual and synoptic analyses in the tropical Atlantic region.

The first part of this research was devoted to studying the interannual variability of cyclonic activity in the tropical Atlantic. The study identified two distinct periods of cyclonic activity, characterized by years of high and low cyclonic activity. It revealed an interaction between cyclonic activity and the characteristics of the monsoon, and the model was found to reproduce the monsoon characteristics quite accurately. However, results are more accurate at the surface than in the upper troposphere, quantitatively proven by mean absolute errors being less important from the surface to the high troposphere.

The second part of this work focused on the ability of the LMDZ model to reproduce the determining parameters of the synoptic scale. The model demonstrated a fairly accurate reproduction of the trajectory and intensity distribution of Hurricane Karl in the tropical Atlantic, from its genesis to dissipation. It showed good performance in simulating various parameters in the lower, middle, and upper troposphere. On the other hand, the model was noted to have limitations in capturing the genesis phase of tropical disturbances, indicating potential areas for improvement. It also exhibited a faster translation speed compared to ERAI.

The study provides valuable insights into the LMDZ model's capabilities in simulating cyclonic activity and underlines its potential for further refinement and application in the field of tropical cyclone research. In the led-up to further assess and enhance the model's performance, those results can be improved by expanding the number of cases studied to improve robustness. Also, it would be very interesting to further investigate dynamic and thermodynamic parameters of the ocean in the Main Development Region (MDR) where cyclonic activity has a significant impact. Further refinement and improvement of the model's parametrizations in capturing the genesis stage of tropical cyclones could be an area for future development and research.

## CONFLICT OF INTERESTS

The authors have not declared any conflict of interests.

## ACKNOWLEDGEMENTS

The authors thank Frederic Hourdin (LMD/CNRS, France) for providing LMDZ simulations, the ANR project

ACASIS and the JEAI IRD program through JEAI-CLISAS (Jeune Equipa Associée à l'IRD-Climat et Santé au Sénégal) for funding this research.

## REFERENCES

- Baek S, Boucher O, Dassas K, Escribano J, Fita L, Forget F, Gainusa-Bogdan A, Guez L, Hourdin C, Hourdin F, Idelkadi A, Lefebvre MP, Li L, Lott F, Madeleine JB, Millour E, Risi C, Sadoury R, Van Phu L (2014). LMDZ5: A documentation, Laboratoire de Meteorologie Dynamique (LMD) 118 p.
- Beven J (2004). Tropical Cyclone Report Hurricane Karl 16-24 September 2004. Technical report. National Hurricane Center, Miami USA 9 p.
- Burpee RW (1972). The origin and structure of easterly waves in the lower troposphere of North Africa. *Journal of the Atmospheric Sciences* 29(1):77-90.
- Camara M (2006). Cyclogenèse dans l'Atlantique Nord en relation avec le système de mousson en Afrique de l'Ouest. Thèse de doctorat, Institut National Polytechnique De Grenoble, Grenoble 240 p.
- Chauvin F, Royer JF, Déqué M (2006). Response of hurricane-type vortices to global warming as simulated by ARPEGE-Climat at high resolution. *Climate Dynamics* 27:377-399.
- Chen TC (2006). Characteristics of African Easterly Waves Depicted by ECMWF Reanalyses for 19912000. *Monthly Weather Review* 134(12):3539-3566.
- Dee DP, Kallen E, Simmons AJ, Haimberger L (2011). Comments on 'Reanalyses suitable for characterizing long-term trends' *Bulletin of the American Meteorological Society* 92:65-72.
- DeMaria M, Knaff JA, Connell BH (2001). A tropical cyclone genesis parameter for the tropical Atlantic. *Weather and Forecasting* 16(2).
- Diallo FB (2012). Rôles des processus couplés convection/surface sur les bilans énergétiques en Afrique de l'ouest. Rapport de stage de 2eme année du Master de dynamique des fluides. Laboratoire de Météorologie dynamique.
- Diedhiou A, Janicot S, Viltard A, De Felice P, Laurent H (1999). Easterly wave regimes and associated convection over West Africa and tropical Atlantic: results from the NCEP/NCAR and ECMWF reanalyses. *Climate Dynamics* 15(11):795-822.
- Diedhiou A, Janicot S, Viltard A, De Felice P (2001). Composite patterns of easterly disturbances over West Africa and the tropical Atlantic: A climatology from the 1979–95 NCEP/NCAR reanalyses. *Climate Dynamics* 18(3):241-253.
- Dieng AL (2015). Etude de la cyclogenèse au large des côtes ouest africaines aux échelles synoptiques et saisonnières. Thèse de Doctorat, Ecole Supérieure Polytechnique de Dakar, 151 p.
- Fink AH, Reiner A (2003). Spatiotemporal variability of the relation between African Easterly Waves and West African Squall Lines in 1998 and 1999. *Journal of Geophysical Research: Atmospheres* 108(D11):4332.
- Goldenberg SB, CW Landsea, AM Mestas-Nunez, WM Gray (2001). The recent increase of Atlantic hurricane activity: Causes and implications. *Science* 293:474-479.
- Hourdin F, Musat I, Bony S, Braconnot P, Codron F, Dufresne JL, Fairhead L, Filiberti MA, Friedling-stein P, Grandpeix JY, Krinner G, LeVan P, Li ZX, Lott F (2006). The lmdz4 general circulation model: climate performance and sensitivity to parametrized physics with emphasis on tropical convection. *Climate Dynamics* 27(7-8):787-813.
- Jenkins GS, Brito E, Soares E, Chiao S, Lima JP, Tavares B, Monteiro M (2017). Hurricane Fred (2015). Cape Verde's First Hurricane in Modern Times: Observations, Impacts, and Lessons Learned. *Bulletin of the American Meteorological Society* 98:2603-2618.
- Landsea CW (1993). A Climatology of Intense (or Major) Atlantic Hurricanes. *Monthly Weather Review* 121(6):1703-1713.
- Lorck J (2019). Dorian: comment la stagnation aggrave les dégâts des ouragans. *Monthly Weather Review* P 10.
- Ohfuchi W, Nkamura H, Yoshioka M, Enomoto T, Takaya K (2004). 10-km mesh meso-scale resolving global simulations of the atmosphere

- on the Earth Simulator — Preliminary outcomes of AFES (AGCM for the Earth Simulator). *Journal of Earth Simulation* 1:8-34.
- Oouchi K, Yoshimura J, Ypshimura H, Mizuta R (2006). Tropical cyclone climatology in a global-warming climate as simulated in a 20 km-mesh global atmospheric model: frequency and wind intensity analysis. *Journal of the Meteorological Society of Japan* 84:259-276.
- Pohl B (2017). *La modelisation numerique du climat*, Centre de Recherches de Climatologie, Biogeosciences, CNRS / UBFC 147p.
- Pytharoulis I, Thorncroft C (1999). The low-level structure of African easterly waves in 1995. *Monthly Weather Review* 127(10):2266-2280.
- Rio C, Hourdin F (2008). A thermal plume model for the convective boundary layer: Representation of cumulus clouds. *Journal of the Atmospheric Sciences* 65:407-425.
- Rio C, Hourdin F, Grandpeix JY, Lafore JP (2009). Shifting the diurnal cycle of parameterized deep convection over land. *Geophysical Research Letters* 36:L07809.
- Sall SM, Sauvageot H (2005). Cyclogenesis off the African Coast: The Case of Cindy in August 1999. *Monthly Weather Review* 133(9):2803-2813.
- Sane Y (2011). Représentation du cycle de vie des systems convectifs dans le modèle LMDz pendant la campagne AMMA 2006. Thèse de doctorat, Université Pierre et Marie Curie 206 p.
- Senghor H, Machu É, Hourdin F, and Gaye AT (2017). Seasonal cycle of desert aerosols in western Africa: analysis of the coastal transition with passive and active sensors. *Atmospheric Chemistry and Physics* 17:8395-8410.
- Shen BW, R Atlas, JD Chern, O Reale, SJ Lin (2006). The 0.125 degree finite-volume general circulation model on the NASA Columbia supercomputer: Preliminary simulations of mesoscale vortices. *Geophysical Research Letters* 33(5).
- Weinkle J, Landsea C, Collins D, Musulin R, Crompton RP, Klotzbach PJ, Pielke R (2018). Normalized hurricane damage in the continental United States 1900-2017. *Nature Sustainability* 1:808-813.